Journal of Materials Chemistry B

Accepted Manuscript

ROYAL SOCIETY OF CHEMISTRY

www.rsc.org/materialsB

Journal Name

RSCPublishing

ARTICLE

Ultrastable green fluorescence carbon dots with high quantum yield for bioimaging and use as theranostic carriers

Chuanxu Yang*, Rasmus Peter Thomsen, Ryosuke Ogaki, Jørgen Kjems and Boon M. Teo*

Cite this: DOI: 10.1039/x0xx00000x

Received 00th January 2012,
Accepted 00th January 2012

DOI: 10.1039/x0xx00000x

www.rsc.org/

Carbon dots (Cdots) have recently emerged as a novel platform of fluorescent nanomaterials. These carbon nanoparticles have great potential in biomedical applications such as bioimaging as they exhibit excellent photoluminescence properties, chemical inertness and low cytotoxicity in comparison to widely used semiconductor quantum dots. However, it remains a great challenge to prepare highly stable, water-soluble green luminescent Cdots with high quantum yield. Herein we report a new synthesis route for green luminescent Cdots imbuing these desirable properties and demonstrate their potential in biomedical applications. Oligoethylenimine (OEI)/β-cyclodextrin (βCD) Cdots were synthesised by a simple and fast heating method in phosphoric acid. The synthesized Cdots showed strong green fluorescence under UV excitation with 30% quantum yield and exhibited superior stability over a wide pH range. We further assembled the Cdots into nanocomplexes with hyaluronic acid for potential use as theranostic carriers. After confirming that the Cdot nanocomplexes exhibited negligible cytotoxicity with H1299 lung cancer cells, in vitro bioimaging of the Cdots and nanocomplexes was carried out. Doxorubicin (Dox), an anticancer drug, was also loaded into the nanocomplexes and the cytotoxicity effect of Dox loaded nanocomplexes with H1299 lung cancer cells was evaluated. Thus, this work demonstrates the great potential of the novel OEI/βCD Cdots in bioimaging and as theranostic carriers.

Introduction

The importance of fluorescent nanomarkers in biomedical applications is rapidly increasing in line with advancements in diagnostic imaging and nanotechnology. Accordingly, much effort has been spent on developing benign fluorescent nanomarkers that can be used for studying intracellular transport and biochemical interactions, and which ultimately can be used for disease detection and therapy. Sun and co-workers were the first to discover that laser-ablated, amorphous carbon nanoparticles can emit in the visible spectral range upon surface functionalisation with polymer chains.[1] These carbon nanoparticles, generally referred to as carbon dots (Cdots) have demonstrated significant potential as a new class of photoluminscent nanoparticles. In comparison with traditional semiconductor-based quantum dots, Cdots have the advantage of being chemically inert and having versatile surface chemistry and potentially low cytotoxicity. Cdots have been demonstrated to possess high quantum yields,[2] nontoxicity,[3-5] nonblinking,[1, 2] and photostability (without photoblinking and photobleaching)[1, 5, 6] properties. Consequently, they are highly competitive in performance in comparison to commercially available CdSe/ZnS quantum dots. Cdots also have been shown to be excellent electron donors, acceptors and, as a result, they offer great promise for a variety of applications, such as light-emitting diodes (LEDs)[7, 8], sensors,[9-11] surface-enhanced Raman scattering (SERS)[12, 13]and biomedical imaging.[9, 14] Generally, the preparation of the Cdots is classified into two groups: top down and bottom up approaches.[15] The top down method, which generally forms Cdots through post treating carbon particles broken down from a larger carbon structure, includes laser ablation,[1] arc discharge[16] and electrochemical oxidation.[17-19] The bottom up approach includes thermal carbonisation,[20] acid dehydration,[6, 21] microwave[22, 23] and ultrasonic treatment,[24] whereby the Cdots are obtained from suitable molecular precursors. The approaches mentioned above often involve complex processes, high energy consuming devices and/or long synthesis times. Moreover, the Cdots obtained from these methods generally exhibit blue luminescence. In the case of bio-imaging, Cdots with blue luminescence are less desirable as optical nanomarkers due to autofluorescence and green luminescent Cdots are considerably more attractive. While blue fluoresecence Cdots have been reported to have quantum yield as high as 80%,[25] the quantum yield of green Cdots have been reported to have relatively low quantum yield.[26-32] Therefore, it remains a challenge to prepare

highly stable, water-soluble green luminescent Cdots with high quantum yield.

As an amino-rich cationic polyelectrolyte, polyethylenimine has been used by several groups for the fabrication of photoluminescent Cdots. In particular, Liu et al. synthesized multicoloured Cdots based on high molecular weight PEI via the microwave pyrolysis method.[33] They further assembled the Cdots into nanocomplexes via electrostatic interactions with DNA for gene delivery applications. However, the use of high molecular weight PEI has shown to be more toxic than its low molecular weight equivalent.[34, 35] Herein, we present for the first time a one-step chemical oxidation scheme for the preparation of highly stable, biocompatible green fluorescent Cdots using low molecular weight branched oligoethylenimine (OEI) as a passivating agent and β-cyclodextrin (βCD) as a carbon source. Specifically, we have (i) synthesised and characterised green fluorescent OEI-βCD carbon dots, (ii) identified the optimal conditions for nanocomplex assembly, (iii) demonstrated the biocompatibility of these Cdots for successful biomedical applications such as cell labelling and imaging and (v) evaluated the cytotoxicity effect of Doxorubicin (Dox) loaded nanocomplexes with H1299 cancer cells (Figure 1).

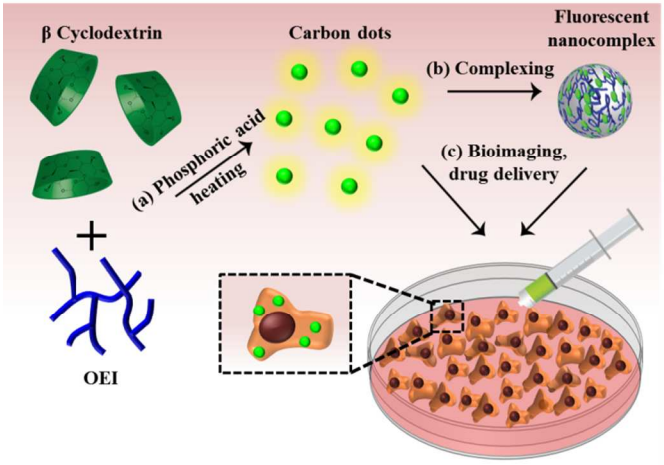

Figure 1. Cartoon illustration of (a) the preparation procedure of green fluorescent Cdots by a simple heating method in phosphoric acid, (b) formation of nanocomplexes with HA, and (c) bioimaging and drug delivery applications with H1299 lung cancer cells.

Experimental Section

Materials. Phosphoric acid (H_3PO_4, 85%), β-cyclodextrin (βCD), fluorescein and sodium hydroxide were purchased from Sigma Aldrich. Low molecular weight polyethylenimine (OEI, 600 Da) was purchased from Alfa Aesar. Hyaluronic acid (HA, 200 kDa) was provided by Lifecore Biomedical (Chaska, MN). Ultrapure water (18.1 MΩ cm, Holm and Halby, Brøndby, Denmark) was used for all experiments.

Synthesis of Cdots. Cdots were synthesized as follows. 100 mg βCD and 50 mg OEI were dissolved in 200 µL of ultrapure water. Then, 300 µL of 85% H_3PO_4 was added and the solution was kept at 90 °C without stirring for 2 h and cooled down to ambient temperature (25 °C). The solution was neutralised with NaOH and then dialysed in ultrapure water through a dialysis membrane (MWCO = 3.5 kDa, Spectra/Por) to remove salt and unreacted compounds. For preparation of Cdots with different composite, predetermined amount of OEI was added into the reaction under the same conditions.

Quantum yield (QY) measurement. The QY of the Cdots was calculated by comparing the integrated fluorescence intensity (excited at 360 nm) and absorbance at 360 nm with those of fluorescein (QY = 79%).[36] To prevent re-absorption, Cdots and fluorescein solutions were diluted such that the absorbance at the excitation wavelength was below 0.1. The QY of the Cdots was calculated according to the following equation:

$$QY_{C\text{-}dots} = QY_{ST} \times \left(\frac{Grad_{C-dots}}{Grad_{ST}}\right) \times \left(\frac{\eta_{C-dots}}{\eta_{ST}}\right)^2$$

where ST denotes the standard, Grad is the gradient from the plot of the integrated photoluminscence intensity vs absorbance, and η (1.33) is the refractive index of the solvent.

Preparation of Cdot-HA nanocomplexes. Cdot-HA nanocomplex was assembled through electrostatic interactions. HA was dissolved in acetate buffer (20 mM, pH = 5.5) at 1 mg/mL overnight and the solution was filtered through 0.2 µm Minisart® syringe filters. HA solution was mixed with the Cdot solution at ratio of 1:30 (w/w) by vortexing and the mixture was incubated for 30 min at room temperature.

To prepare Dox loaded nanocomplexes, a solution of Dox (5 mg/ml) was first mixed with Cdots solution with the weight ratio of 1: 3, which was further added into hyaluronic acid solution at the ratio of Cdots: HA of 1:30 (w/w). The mixture was incubated for 30 min before purified using centrifugal filter units (3,000 MWCO, Amicon Ultra) to remove unencapsulated Dox, which was quantified by measuring the fluorescent intensity at λex 480 nm and λem 590 nm (FLUOstar OPTIMA, Moritex BioScience). The encapsulation efficiency (EE) was calculated as follows: EE (%)= 100 × (total Dox – unencapsulated Dox)/total Dox.

Characterisation. The absorption spectra of the Cdots in ultrapure water were measured with a NanoDrop ND-1000 spectrophotometer (Nanodrop, Wilmington, DE, USA). The fluorescence emission spectra of the Cdot solution were recorded using a Horiba Join Yvon Fluoromax-3 fluorimeter. The fluorescence spectra of the Cdots at different pH values at the same concentration were also recorded.

Fourier transform infrared (FTIR) spectroscopy was used to analyse possible chemical bonds existing in the Cdots. The purified Cdots were freeze-dried and loaded to the sample disc and analysed using a Perkin-Elmer Paragon 1000 FTIR spectrometer.

The morphology of the Cdots and the Cdot-HA complex were examined by liquid tapping-mode atomic force microscopy (AFM) imaging using an Agilent 5500 AFM and a Bruker silicon nitride probe Model OTR4-10 with a spring constant of 0.02 N/m. The morphologies of both Cdots and nanocomplexes

were also observed using a transmission electron microscope (TEM, FEI Tecnai G2 Spirit).

The size distribution of the Cdots and nanocomplexes were characterised by photon correlation spectroscopy (PCS) and zeta potential was measured by laser Doppler velocimetry (LDV) at 25 °C using a Zetasizer Nano ZS (Malvern Instruments, Malvern, UK).

X-ray Photoelectron Spectroscopy (XPS) data acquisition was performed using a Kratos Axis Ultra DLD instrument (Kratos Analytical Ltd., Telford, U.K.) equipped with a monochromated Alkα X-ray source (hν = 1486.6 eV) operating at 15 kV and 10 mA (150 W). Survey spectra (binding energy (BE) range of 0–1100 eV with a pass energy of 160 eV) were used for element identification and quantification. High resolution C 1s spectra were acquired with a pass energy of 20 eV. The acquired data were converted to VAMAS format and analyzed using CasaXPS (Casa Software Ltd., U.K.) software. Three separately prepared samples were analyzed. All spectra were calibrated to C-C/C-H at the binding energy of 285 eV.

Photostability and thermal stability study. To test the photostability, Cdots and FITC solutions were exposed to continuous laser illumination at excitation of 488 nm for a designated period. The fluorescence intensity of each sample was measured and normalised to their initial value.

For thermal stability test, a standard 5 Amp analog temperature controller (Wavelength Electronics, Model-LFI-3751) was connected to the fluorimeter for precise adjustment of the sample temperature during the measurement.

Cell culture. H1299 lung cancer cells were obtained from American Type Culture Collection, Denmark (ATCC). Cells were maintained in RPMI medium supplemented with 10% fetal bovine serum (FBS) and 1% penicillin-streptomycin at 37 °C in 5% CO2 and 100% humidity.

Cytotoxicity assay. The cytotoxicity of the Cdots was evaluated by an AlamarBlue assay (Molecular Probes, Life Technologies) according to manufacturer's protocol. Cells were seeded in a 96-well plate at a density of 5×10^4/well in 100 µL medium for 24 h. The medium was replaced with 100 µL fresh medium containing Cdots at different concentrations (0–1 mg/mL). After 24 h incubation, the cells were rinsed with PBS and treated with AlamarBlue reagent (10% in medium) for 2 h. The fluorescent intensity of the medium was measured using a plate reader (FLUOstar OPTIMA, Moritex BioScience) at an excitation wavelength of 540 nm and emission wavelength of 590 nm.

Cell imaging. Cells were seeded in 8-well tissue culture chambers (SARSTED, Germany) at a density of 5×10^4/well for 24 h. The medium was then replaced with a fresh medium containing Cdots (500 µg/mL) or the Cdot-HA nanocomplexes. After 4 h incubation, the cells were washed with PBS and fixed with 4% paraformaldehyde for 15 min at room temperature. The cell membranes were stained with Concanavalin A, Alexa Fluor 647 conjugate (Molecular Probes). The fluorescent images were recorded using Olympus X81microscope.

***In vitro* anti-tumor experiment.** H1299 cells were seeded in 96-well plate as previously. After incubation overnight, the medium was replaced with 100 µL fresh medium containing free Dox or nanocomplex-Dox with different concentrations, ranging from 0.1 µM - 1µM. The cells were incubated for another 48 h before analysed by AlamarBlue assay.

Results and Discussion

Synthesis and characterisation of Cdots

There have been several recent studies demonstrating the use carbohydrates as the main carbon source for the synthesis of Cdots. While a detailed mechanism remains to be identified, it has been postulated that carbohydrates first undergo hydrolysis and dehydration, followed by decomposition in the presence of acid to generate soluble moieties such as aldehydes, ketones, with further polymerisation and condensation resulting in the formation of soluble polymeric products.[37-39] Cdots are finally formed by aromatisation and carbonisation. In the present study, Cdots with green fluorescence were obtained through carbonisation of OEI and cyclodextrin via a one-step heating procedure in phosphoric acid. The addition of concentrated phosphoric acid assisted in the dehydration and carbonisation of OEI-CD. It should be noted that the heating of pure OEI and pure cyclodextrin did not yield fluorescent Cdots (Figure S1); this was only achieved by heating mixtures of OEI and CD. This results points to nitrogen-doped Cdots enhancing the fluorescence, as has been observed by several other research groups.[39, 40]

The obtained brownish yellow sample was diluted for AFM characterisation to determine the size distribution of the synthesized Cdots. The AFM image in Figure 2a and TEM image in Figure 2c confirm that the Cdots were well-dispersed, spherical nanodots and the height profile (Figure 2b) indicated uniform sizes of approximately 2–4 nm, which is in good agreement with previous reports.[9, 20, 25, 40]

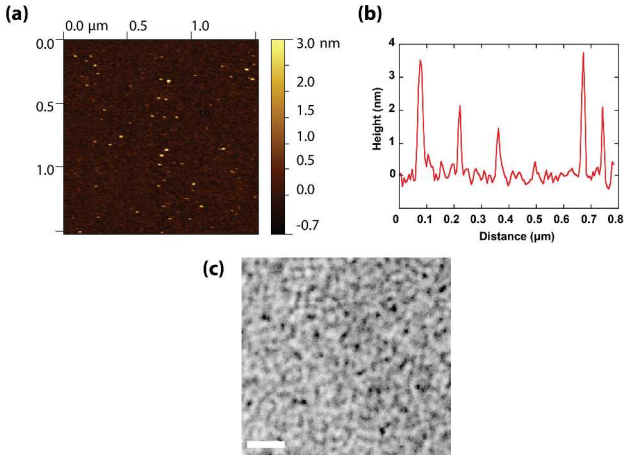

Figure 2. a) AFM image, b) height profile and c) TEM image of Cdots, scalebar= 20 nm.

The composition and functional groups of the Cdots were analysed using FTIR. Figure 3a shows the FTIR spectra of pure OEI, pure βCD and OEI-βCD Cdots. The broad band observed at 3330 cm^{-1} suggests the existence of O-H and N-H, while the

peak at 1800 cm^{-1} is attributed to anhydride C=O of βCD. The new peaks at 1650 cm^{-1} can be attributed to the amide I C=O and NO_2 and the increased intensity of the peak at 2300 cm^{-1} represents the aldehyde C-H, suggesting that the OEI molecules were grafted onto the surface of the Cdots. To further examine the elemental composition of the Cdots, XPS measurements were performed. Figure 3b shows the XPS survey scan of the Cdots and clearly reveals the presence of carbon, nitrogen, oxygen and phosphorus. The high resolution C1s XPS spectrum were fitted and assigned into five peaks at the binding energies (BE) of 285 eV (C-C/C-H), ~286.2 eV (C-N), ~286.8 eV (C-O), ~288 eV (C=O/N-C=O) and ~289.5 eV (C(=O)-O) while the N1s XPS spectrum were assigned to the corresponding peaks at binding energies (BE) of 402 eV (NH_3^+), 400 eV (C-N/N-C(=O) and ~405 eV (NO_2).[41] Analysis of the elemental composition as shown in Table S1, with 36.8% carbon, 46.7 % oxygen, 7.8% nitrogen and 8.7 % phosphorus indicate that the Cdots are nitrogen and phosphorus doped.

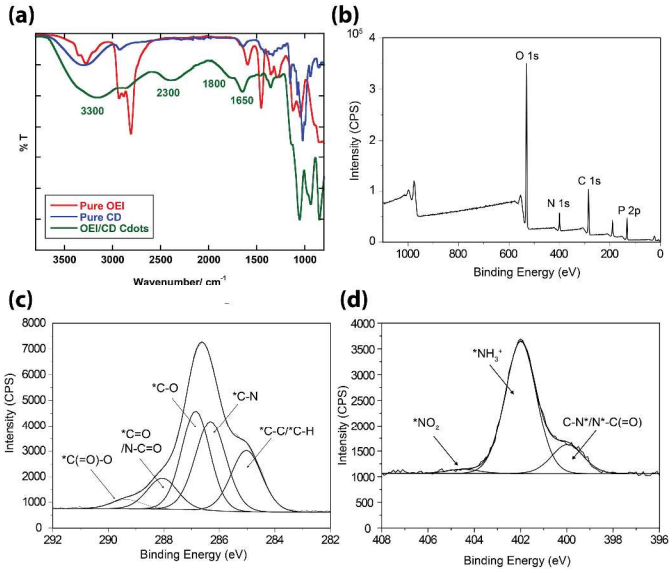

Figure 3. a) FTIR of pure OEI, pure CD and OEI/CD Cdots, b) XPS survey scan of Cdos and c) XPS high resolution survey scan of C1s.

To study the optical properties of the Cdots, UV–vis and fluorescence spectra were analysed. The UV–vis spectrum of the Cdots in Figure 4a reveals a strong absorption band peak at approximately 280 nm and a shoulder peak around 320 nm. The peak at 280 nm was attributed to the blue-shifted π–π* transition of the conjugated C=C units from the carbon core and the shoulder peak at 320 nm was attributed to the n–π* transition of C=O groups on the surface of the Cdots.[39]The slight shoulder peak at 350 nm is attributed to the presence of aromatic π orbitals of larger Cdots.[42]

The diluted aqueous dispersion of OEI/βCD Cdots under normal light appeared light yellowish and remained stable for several weeks with no signs of aggregation (Figure 4a, inset). Upon excitation under a 365-nm UV lamp, the Cdots emitted strong green luminescence with a quantum yield of approximately 30%, estimated using fluorescein as the reference (Figure S2a). The current ratio of βCD to OEI (2:1) was chosen to optimise the quantum yield of the as prepared Cdots (Figure S2b) while keeping the amount of OEI minimum in consideration of biocompatibility. Here, OEI was used as the passivating agent as it is generally well known that employing the surface passivation method whereby an organic component, such as an amine to introduce emissive energy traps to allow the emissive recombination of localised electron hole pairs, can assist in increasing the quantum yield of the fluorescent probe.[15, 43] To further explore the optical properties of the OEI/βCD Cdots, fluorescence emission spectra of the prepared Cdots were recorded at various excitation wavelengths from 390 to 470 nm (Figure 4b). It can be seen that with an excitation wavelength of 390 nm, the fluorescence intensity was maximum at 510 nm and further increasing the excitation wavelength resulted in a decrease of the fluorescence intensity. Particularly interesting was that there was only a slight shift of the fluorescence peak from 390 to 470 nm. This indicates that the fluorescence origin of our OEI/βCD Cdots was not excitation wavelength dependent. Importantly, to the best of our knowledge, this is different from all of the Cdots with so-called "multicoloured" fluorescence reported in the literature.[25, 44] The exact mechanism of green fluorescence of the Cdots currently remains under debate; however, it is generally reported that this originates from the formation of special molecule-like states containing carboxyl groups and carbonyl groups in carbon nanodots.[26]

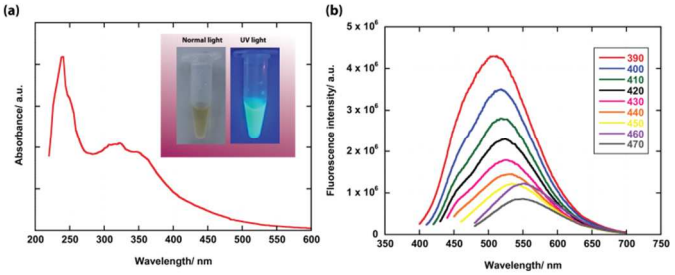

Figure 4. a) UV–vis absorption spectrum of OEI/βCD Cdots (Inset: photographs of OEI/βCD Cdots taken under normal light and UV lamp with an excitation wavelength of 365 nm, respectively) and b) fluorescence spectra of the Cdots with excitation wavelengths from 390 to 470 nm in 10-nm increments.

To verify the pH stability of the Cdots, the fluorescence intensity of the Cdots at different pH values from 1 to 13 was recorded. As shown in Figure 5a,c the fluorescence intensity of the Cdots was very stable over a wide pH range. Only in strongly alkaline solutions did the fluorescence intensity decrease (by approximately 30%). The pH effect implies that the fluorescent species in the Cdots have acidic sites that are associated with the green emission as the fluorescence is quenched in basic media.[45] Interestingly, the fluorescence emission peak did not shift with varying pH (Figure 5b). The stability of our Cdots against changes in pH over a wide range is unique because previously reported Cdots have shown pH-dependent properties.[25, 27, 46] Furthermore, our Cdots also exhibit excellent photostability over a period of two months (data not shown). The excellent pH- and photostability demonstrated makes our fluorescent Cdots promising

candidates for a new class of fluorescence probes for biosensors and biomedical imaging devices.

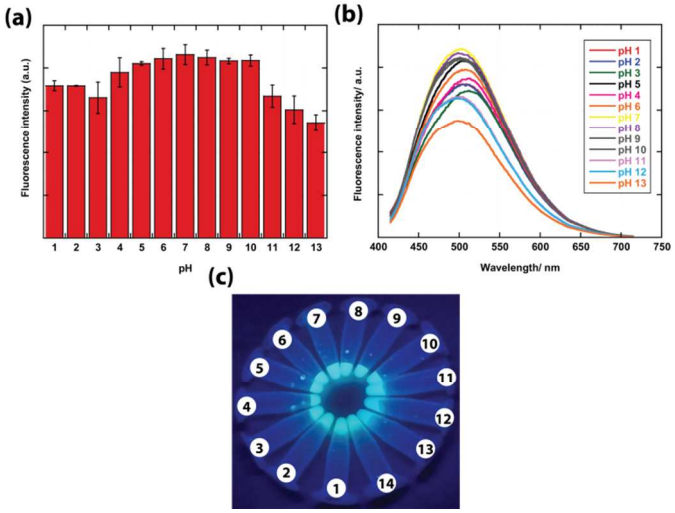

Figure 5. a) Fluorescence intensity changes, b) fluorescence intensity spectra and c) photograph of the Cdots excited with a 365-nm UV lamp in solutions with different pH values.

The stability of fluorescence nanomaterials is an important feature to consider for various applications. Herein, we exposed our Cdots and a commercially available fluorescence dye, fluorescein with a laser excited at 488 nm for various time points. As shown in Figure 6a, the fluorescence intensity of our Cdots after 14 minutes remained stable while the fluorescence intensity of fluorescein only preserved 60% of the initial intensity. In addition to the photo-stability of our Cdots in comparison with fluorescein, the fluorescence intensity of both probes decreased slightly and both retained almost 90% of the initial intensity upon increasing the temperature from 25 to 50 °C (Figure 6b). This points towards the usefulness of our Cdots in *in vivo* temperature sensing applications.

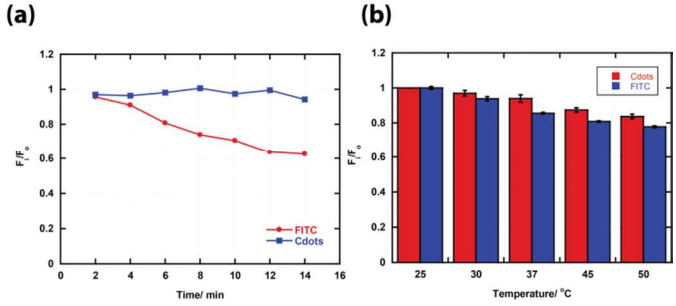

Figure 6. a) Photostability of Cdots and fluorescein irradiated with a laser excited at 488 nm at different time points, b) Stability of Cdots and fluorescein as a function of temperature.

Formation of Cdot-HA nanocomplexes

Nanocomplexes are a promising drug delivery system due to the high loading capacity and the protective effect of biomacromolecules including proteins and nucleic acids. [33, 47-49] Here we demonstrate the potential application of our photoluminescent Cdots as theranostic systems by forming complexes with negative charged macromolecules. As illustrated in Figure 1, the branched OEI/CD functionalised Cdots can form nanocomplexes with HA through electrostatic interactions between the positively charged primary amine groups on the surface of the Cdots and negatively charged carboxyl groups of HA. We optimised the ratio between the OEI/βCD Cdots and HA to form the nanosized complexes. The average size of the nanocomplexes was determined by AFM and DLS. As shown in the AFM and TEM images in Figures 7a,b the nanocomplexes formed are approximately 250 nm in size. The corresponding hydrodynamic diameters of the nanocomplexes shown in Figure 7c are in good agreement with the AFM results. The efficient complexation also suggests the strong binding ability of the Cdots to HA. This is also further confirmed by zeta potential measurements of the Cdots and Cdot-HA complexes (Figure S4).

Cell imaging

To demonstrate the potential of the Cdots and nanocomplexes as fluorescent markers and theranostic carriers for therapeutic payloads, respectively, they were applied directly for the imaging of H1299 lung cancer cells without further functionalisation. Figure 8 shows the optical and fluorescence images of (a) cells as controls, (b) cells incubated with Cdots and (c) cells incubated with Cdot nanocomplexes for 4 h. It should be noted that the concentration of the Cdots used for complexation with HA was 0.5 mg/mL for the comparison of cellular association/uptake of the Cdots and nanocomplexes (Figure S3). Cells that were incubated with Cdots and Cdot nanocomplexes emitted green luminescence upon 405 nm excitation, whereas no green fluorescence was detected in the control cells (without incubation with Cdots) under the same conditions. Furthermore, there were no remarkable differences in the fluorescence intensity of the cells when incubated with Cdots and Cdot nanocomplexes. This thereby demonstrates our OEI/βCD Cdots with distinctive green luminescence possess great promise in serving as fluorescence markers for bio-imaging applications.

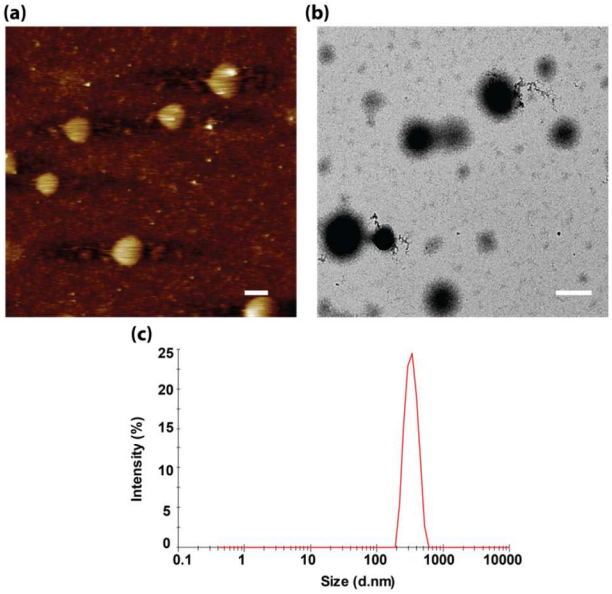

Figure 7. a) AFM image and b) TEM image of OEI/βCD Cdots complexes, scalebar: 200 nm; c) hydrodynamic diameter of the nanocomplexes.

Apart from the bright luminescence and high stability mentioned above, our Cdots also exhibited negligible cytotoxicity. Incubating the cells for 24 h in up to 1 mg/mL of the Cdots did not weaken the cell activity significantly (Figure 9).

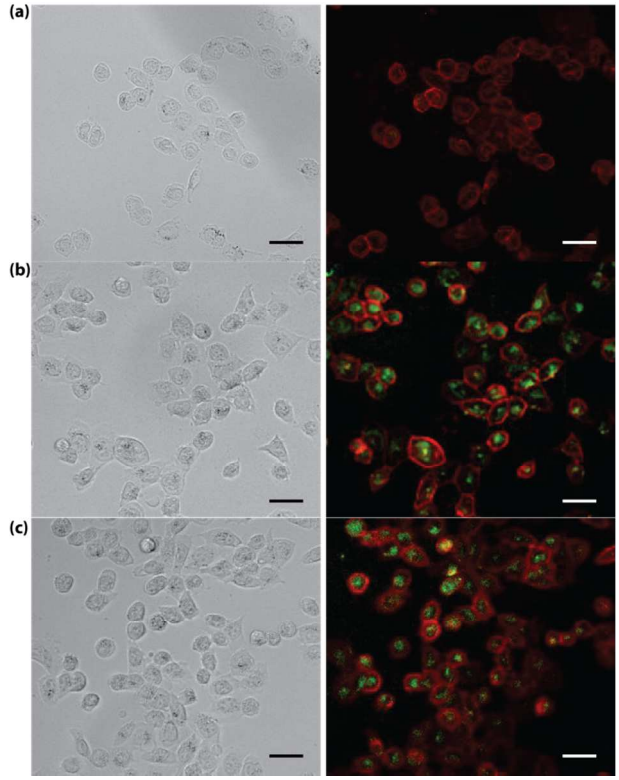

Figure 8. Bright field and fluorescence images of a) cells only, b) cells incubated with Cdots and c) cells incubated with nanocomplexes for 4 h. Scalebar: 20 µm.

To further demonstrate that our cdots nanocomplexes can be utilized for drug delivery purposes, doxorubicin (Dox), a commonly used anticancer drug, was loaded into the nanocomplexes. The encapsulation of Dox within the nanocomplexes is driven by the electrostatic interaction of positively charged Dox and Cdots and negatively charged HA. The loading capacity of Dox was approximately 34.1 % and DLS analysis of Dox encapsulated nanocomplexes was further performed to confirm the formation of nanocomplexes (Figure S5). The nanocomplexes with Dox encapsulated were approximately 373.6 nm in size and a PDI of 0.123. The cytotoxicity effect of the Dox encapsulated nanocomplexes against lung cancer cells were studied and as shown in Figure 10, similar to the free Dox, the cytotoxicity of the Dox encapsulated nanocomplexes showed a dose dependent increase with increasing Dox concentration. Particularly, Dox loaded nanocomplexes exhibit statistically significant higher cytotoxicity than free Dox. This results point to the easier uptake of Dox loaded nanocomplexes via endocytosis pathway by lung cancer cells as compared to the passive diffusion of free Dox molecules.

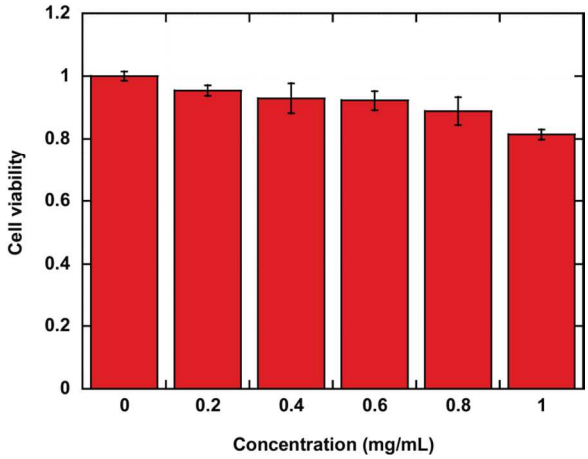

Figure 9. Viability of H1299 lung cancer cells with different concentrations of Cdots

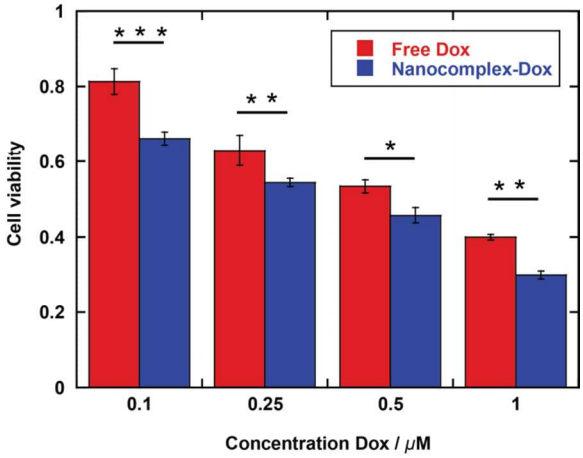

Figure 10. Cell viability of H1299 cells incubated with free Dox and Dox loaded nanocomplexes. Results are mean ± SD, *p < 0.05, *p< 0.01 and *p<0.0001.

Nanocomplexes for DOX delivery

Conclusions

In summary, we have successfully demonstrated a simple one-pot synthesis of highly stable, green luminescent Cdots based on OEI, βCD and phosphoric acid precursors. The Cdots exhibited excellent photoluminescent properties and showed good stability over a wide pH range. Furthermore, the synthesized Cdots exhibited negligible cytotoxicity to lung cancer cells and fluorescence images of the cells incubated with the Cdots and Cdot nanocomplexes demonstrated that they could be efficiently taken up by the cells. Furthermore, our Dox loaded Cdots based nanocomplexes showed enhanced cytotoxicity effect towards lung cancer cells than free Dox. The simple synthesis method developed in this work also paves the way for several promising applications in light-emitting diodes, cellular imaging and theranostic agents.

Acknowledgements

This work was supported by the Lundbeck Foundation and the Danish Council for Independent Research, Technology and Production Sciences, Denmark. We are grateful to Prof. Kurt Gothelf at the Interdisciplinary Nanoscience Center (iNANO), Aarhus University for kindly granting the use of their lab facilities.

Notes and references

[a] Interdisciplinary Nanoscience Center (iNANO)
The iNANO House
Gustav Wieds Vej 14
Aarhus University
DK-8000 Aarhus C
Email:chuanxuyang@inano.au.dk, bteo@inano.au.dk

Electronic Supplementary Information (ESI) available: [Figure S1 to S4: .Figure S1: a) Photographs of (i) water, (ii) processed OEI, (iii) processed βCD and (iv) OEI/βCD Cdots under a UV lamp excited at 365 nm, b) fluorescence intensity of OEI, βCD and OEI/βCD Cdots using an excitation wavelength of 400 nm, Figure S2: a) Integrated fluorescence intensity vs. absorbance fluorescence spectrum of the Cdots and OEI/CD complex, b) quantum yield of Cdots as a function of ratio of βCD/OEI. Figure S3: a) Photographs of (i) water, (ii) OEI/βCD Cdots and (iii) OEI/βCD complex under normal light and a UV lamp excited at 365 nm. b) fluorescence spectrum of the Cdots and OEI/CD complex, excitation wavelength 400 nm, Figure S4: Zeta potential of a) Cdots and b) nanocomplex, Figure S5: Particle size of Dox loaded nanocomplex. Tab;e S1: Elemental composition of Cdots as determined by XPS measurements. See DOI: 10.1039/b000000x/

1. Y.-P. Sun, B. Zhou, Y. Lin, W. Wang, K. A. S. Fernando, P. Pathak, M. J. Meziani, B. A. Harruff, X. Wang, H. Wang, P. G. Luo, H. Yang, M. E. Kose, B. Chen, L. M. Veca and S.-Y. Xie, *Journal of the American Chemical Society*, 2006, 128, 7756-7757.
2. R. Liu, D. Wu, S. Liu, K. Koynov, W. Knoll and Q. Li, *Angewandte Chemie International Edition*, 2009, 48, 4598-4601.
3. X. Huang, F. Zhang, L. Zhu, K. Y. Choi, N. Guo, J. Guo, K. Tackett, P. Anilkumar, G. Liu, Q. Quan, H. S. Choi, G. Niu, Y.-P. Sun, S. Lee and X. Chen, *ACS Nano*, 2013, 7, 5684-5693.
4. H. Tao, K. Yang, Z. Ma, J. Wan, Y. Zhang, Z. Kang and Z. Liu, *Small*, 2012, 8, 281-290.
5. Q.-L. Zhao, Z.-L. Zhang, B.-H. Huang, J. Peng, M. Zhang and D.-W. Pang, *Chemical Communications*, 2008, DOI: 10.1039/B812420E, 5116-5118.
6. H. Peng and J. Travas-Sejdic, *Chemistry of Materials*, 2009, 21, 5563-5565.
7. X. Guo, C.-F. Wang, Z.-Y. Yu, L. Chen and S. Chen, *Chemical Communications*, 2012, 48, 2692-2694.
8. X. Zhang, Y. Zhang, Y. Wang, S. Kalytchuk, S. V. Kershaw, Y. Wang, P. Wang, T. Zhang, Y. Zhao, H. Zhang, T. Cui, Y. Wang, J. Zhao, W. W. Yu and A. L. Rogach, *ACS Nano*, 2013, 7, 11234-11241.
9. C. Shen, Y. Sun, J. Wang and Y. Lu, *Nanoscale*, 2014, 6, 9139-9147.
10. W. Shi, Q. Wang, Y. Long, Z. Cheng, S. Chen, H. Zheng and Y. Huang, *Chemical Communications*, 2011, 47, 6695-6697.
11. L. Zhou, Y. Lin, Z. Huang, J. Ren and X. Qu, *Chemical Communications*, 2012, 48, 1147-1149.
12. H. Cheng, Y. Zhao, Y. Fan, X. Xie, L. Qu and G. Shi, *ACS Nano*, 2012, 6, 2237-2244.
13. P. Luo, C. Li and G. Shi, *Physical Chemistry Chemical Physics*, 2012, 14, 7360-7366.
14. L. Cao, X. Wang, M. J. Meziani, F. Lu, H. Wang, P. G. Luo, Y. Lin, B. A. Harruff, L. M. Veca, D. Murray, S.-Y. Xie and Y.-P. Sun, *Journal of the American Chemical Society*, 2007, 129, 11318-11319.
15. S. Y. Lim, W. Shen and Z. Gao, *Chemical Society Reviews*, 2014, DOI: 10.1039/C4CS00269E.
16. M. Bottini, C. Balasubramanian, M. I. Dawson, A. Bergamaschi, S. Bellucci and T. Mustelin, *The Journal of Physical Chemistry B*, 2005, 110, 831-836.
17. L. Zheng, Y. Chi, Y. Dong, J. Lin and B. Wang, *Journal of the American Chemical Society*, 2009, 131, 4564-4565.
18. H. Li, X. He, Z. Kang, H. Huang, Y. Liu, J. Liu, S. Lian, C. H. A. Tsang, X. Yang and S.-T. Lee, *Angewandte Chemie International Edition*, 2010, 49, 4430-4434.
19. H. Ming, Z. Ma, Y. Liu, K. Pan, H. Yu, F. Wang and Z. Kang, *Dalton Transactions*, 2012, 41, 9526-9531.
20. Z. L. Wu, P. Zhang, M. X. Gao, C. F. Liu, W. Wang, F. Leng and C. Z. Huang, *Journal of Materials Chemistry B*, 2013, 1, 2868-2873.
21. X. Wang, K. Qu, B. Xu, J. Ren and X. Qu, *Nano Res.*, 2011, 4, 908-920.
22. X. Wang, K. Qu, B. Xu, J. Ren and X. Qu, *Journal of Materials Chemistry*, 2011, 21, 2445-2450.
23. W. Wei, C. Xu, L. Wu, J. Wang, J. Ren and X. Qu, *Sci. Rep.*, 2014, 4.
24. Z. Ma, H. Ming, H. Huang, Y. Liu and Z. Kang, *New Journal of Chemistry*, 2012, 36, 861-864.
25. S. Zhu, Q. Meng, L. Wang, J. Zhang, Y. Song, H. Jin, K. Zhang, H. Sun, H. Wang and B. Yang, *Angewandte Chemie International Edition*, 2013, 52, 3953-3957.
26. L. Wang, S.-J. Zhu, H.-Y. Wang, S.-N. Qu, Y.-L. Zhang, J.-H. Zhang, Q.-D. Chen, H.-L. Xu, W. Han, B. Yang and H.-B. Sun, *ACS Nano*, 2014, 8, 2541-2547.
27. W. Wang, Y. Li, L. Cheng, Z. Cao and W. Liu, *Journal of Materials Chemistry B*, 2014, 2, 46-48.
28. S. Zhu, J. Zhang, C. Qiao, S. Tang, Y. Li, W. Yuan, B. Li, L. Tian, F. Liu, R. Hu, H. Gao, H. Wei, H. Zhang, H. Sun and B. Yang, *Chemical Communications*, 2011, 47, 6858-6860.
29. J. Zhang, W. Shen, D. Pan, Z. Zhang, Y. Fang and M. Wu, *New Journal of Chemistry*, 2010, 34, 591-593.

30. J. Zhou, P. Lin, J. Ma, X. Shan, H. Feng, C. Chen, J. Chen and Z. Qian, *RSC Advances*, 2013, 3, 9625-9628.
31. Y. Fang, S. Guo, D. Li, C. Zhu, W. Ren, S. Dong and E. Wang, *ACS Nano*, 2011, 6, 400-409.
32. N. Gong, H. Wang, S. Li, Y. Deng, X. a. Chen, L. Ye and W. Gu, *Langmuir*, 2014, 30, 10933-10939.
33. C. Liu, P. Zhang, X. Zhai, F. Tian, W. Li, J. Yang, Y. Liu, H. Wang, W. Wang and W. Liu, *Biomaterials*, 2012, 33, 3604-3613.
34. H. Lv, S. Zhang, B. Wang, S. Cui and J. Yan, *Journal of Controlled Release*, 2006, 114, 100-109.
35. T. Xia, M. Kovochich, M. Liong, H. Meng, S. Kabehie, S. George, J. I. Zink and A. E. Nel, *ACS Nano*, 2009, 3, 3273-3286.
36. J. Q. Umberger and V. K. LaMer, *Journal of the American Chemical Society*, 1945, 67, 1099-1109.
37. S. Sahu, B. Behera, T. K. Maiti and S. Mohapatra, *Chemical Communications*, 2012, 48, 8835-8837.
38. Y. Liu, N. Xiao, N. Gong, H. Wang, X. Shi, W. Gu and L. Ye, *Carbon*, 2014, 68, 258-264.
39. Z. Qian, J. Ma, X. Shan, H. Feng, L. Shao and J. Chen, *Chemistry – A European Journal*, 2014, 20, 2254-2263.
40. H. Ding, J.-S. Wei and H.-M. Xiong, *Nanoscale*, 2014, DOI: 10.1039/C4NR04267K.
41. G. Beamson and D. Briggs, *Journal of Chemical Education*, 1993, 70, A25.
42. W. Kwon and S.-W. Rhee, *Chemical Communications*, 2012, 48, 5256-5258.
43. X. Li, S. Zhang, S. A. Kulinich, Y. Liu and H. Zeng, *Sci. Rep.*, 2014, 4.
44. X. Jia, J. Li and E. Wang, *Nanoscale*, 2012, 4, 5572-5575.
45. Z. Zhang, J. Hao, J. Zhang, B. Zhang and J. Tang, *RSC Advances*, 2012, 2, 8599-8601.
46. C. Yang, S. Gao and J. Kjems, *Journal of Materials Chemistry B*, 2014, DOI: 10.1039/C4TB01374C.
47. Yang C, Nilsson L, Cheema MU, Wang Y, Frøkiær J, Gao S, Kjems J and N. R., *Theranostics* 2015, 5, 110-123.
48. J. E. Chung, S. Tan, S. J. Gao, N. Yongvongsoontorn, S. H. Kim, J. H. Lee, H. S. Choi, H. Yano, L. Zhuo, M. Kurisawa and J. Y. Ying, *Nat Nano*, 2014, advance online publication.
49. L. Wang, X. Wang, A. Bhirde, J. Cao, Y. Zeng, X. Huang, Y. Sun, G. Liu and X. Chen, *Advanced Healthcare Materials*, 2014, 3, 1203-1209.

Table of Contents

Green luminescent carbon dots with high quantum yield and superior stability over a range of pH are synthesized for the first time via a new heating method. The carbon dots can be assembled into defined nanocomplexes, enabling their potential use as benign theranostic carriers for delivery of doxorubicin to cells.

Keyword fluorescence, carbon dots, theranostic carriers, bioimaging, doxorubicin